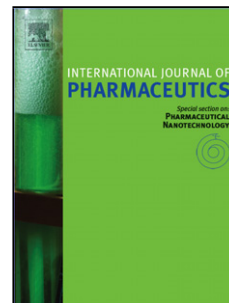


## Accepted Manuscript

Title: Development and characterisation of electrospun timolol maleate-loaded polymeric contact lens coatings containing various permeation enhancers

Authors: Prina Mehta, Ali Al-Kinani, Muhammad Sohail Arshad, Ming-Wei Chang, Raid G Alany, Zeeshan Ahmad



PII: S0378-5173(17)30895-5  
DOI: <http://dx.doi.org/10.1016/j.ijpharm.2017.09.029>  
Reference: IJP 17010

To appear in: *International Journal of Pharmaceutics*

Received date: 3-6-2017  
Revised date: 11-9-2017  
Accepted date: 12-9-2017

Please cite this article as: Mehta, Prina, Al-Kinani, Ali, Arshad, Muhammad Sohail, Chang, Ming-Wei, Alany, Raid G, Ahmad, Zeeshan, Development and characterisation of electrospun timolol maleate-loaded polymeric contact lens coatings containing various permeation enhancers. *International Journal of Pharmaceutics* <http://dx.doi.org/10.1016/j.ijpharm.2017.09.029>

This is a PDF file of an unedited manuscript that has been accepted for publication. As a service to our customers we are providing this early version of the manuscript. The manuscript will undergo copyediting, typesetting, and review of the resulting proof before it is published in its final form. Please note that during the production process errors may be discovered which could affect the content, and all legal disclaimers that apply to the journal pertain.

## Development and characterisation of electrospun timolol maleate-loaded polymeric contact lens coatings containing various permeation enhancers

Prina Mehta<sup>1</sup>, Ali Al-Kinani<sup>2</sup>, Muhammad Sohail Arshad<sup>1</sup>, Ming-Wei Chang<sup>3,4</sup>, Raid G Alany<sup>2</sup> and Zeeshan Ahmad<sup>1\*</sup>

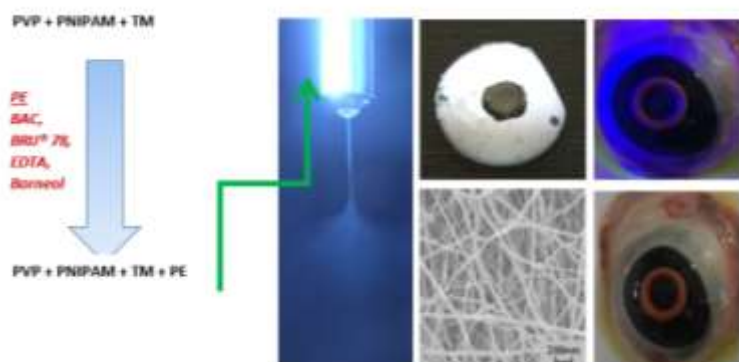
1. Leicester School of Pharmacy, De Montfort University, Leicester, LE1 9BH, UK
2. Kingston University London, School of Pharmacy and Chemistry, Kingston Upon Thames, KT1 2EE, Surrey, UK
3. College of Biomedical Engineering and Instrument Science, Zhejiang University, Hangzhou 310027, China
4. Zhejiang Provincial Key Laboratory of Cardio-Cerebral Vascular Detection Technology and Medicinal Effectiveness Appraisal, Zhejiang University, Hangzhou 310027, China

Corresponding author:

Prof. Z Ahmad: zahmad@dmu.ac.uk

Tel: +44 (0) 116 250 6455

### Graphical abstract



### Abstract

Despite exponential growth in research relating to sustained and controlled ocular drug delivery; anatomical and chemical barriers of the eye still pose formulation challenges. Nanotechnology integration into the pharmaceutical industry has aided efforts in potential ocular drug device development. Here, the integration and in vitro effect of four different permeation enhancers (PEs) on the release of anti-glaucoma drug timolol maleate (TM) from

polymeric nanofiber formulations is explored. Electrohydrodynamic (EHD) engineering, more specifically electrospinning, was used to engineer nanofibers (NFs) which coated the exterior of contact lenses. Parameters used for engineering included flow rates ranging from 8 to 15  $\mu\text{L}/\text{min}$  and a novel EHD deposition system was used; capable of hosting four lenses, masked template and a ground electrode to direct charged atomised structures. SEM analysis of the electrospun structures confirmed the presence of smooth nano-fibers; whilst thermal analysis confirmed the stability of all formulations. *In vitro* release studies demonstrated a triphasic release; initial burst release with two subsequent sustained release phases with most of the drug being released after 24 hours (86.7%) Biological evaluation studies confirmed the tolerability of all formulations tested with release kinetics modelling results showing drug release was via quasi-Fickian or Fickian diffusion. There were evident differences ( $p < 0.05$ ) in TM release dependant on permeation enhancer.

**KeyWords:** Electrospinning; contact lens; coatings; fibers; timolol maleate; glaucoma; permeation enhancer

## Introduction

Despite being an accessible organ, it is the structure of the eye (more specifically the corneal structure) that poses great challenges with respect to ocular drug delivery (Mehta, et al. 2017a; Taskar, et al. 2017). The cornea is a transparent tissue located in anterior of the iris; with a primary function of providing protection to the front of the eye and to focus light entering the eye. The corneal tissue is approximately 500 $\mu\text{m}$  thick and 11mm in diameter. There are three distinct regions to the cornea; endothelium, stroma and epithelium. The endothelium is the inner most layer of the cornea with high porosity allowing the thickness of the cornea to be controlled by hydration. The majority of the cornea is made up of the stroma; a collagen rich layer separated from the endothelium by Descemet's membrane. The Bowmen Layer connects the stroma to the epithelium, the outer most layer of the cornea (Kong and Mi 2016). The composition of these layers results in various degrees of hydrophilicity across the cornea and as a result of this, drug delivery through the cornea is a challenge. There are 2 mechanisms of drug transport through the cornea; paracellular and transcellular. Paracellular transport is restricted to polar molecules due to the hydrophilic stroma and epithelial whilst larger molecules are often halted by tight junctions between

corneal cells. Transcellular drug transport involves partition between hydrophilic (e.g. stroma) and lipophilic (e.g. endothelium) environment.

There are various factors which affect drug permeation through the cornea; all which can be categorised into three groups; physiochemical factors, physiological factors and formulation factors. Physiochemical factors refer to drug properties that interfere with passive diffusion of drug (e.g. partition coefficient of the drug and molecular weight) (Mun, et al. 2014). Physiological barriers focus on pre-corneal factors (dilution due to tear production, pre-corneal volume (25-30 $\mu$ l), corneal tissue components (e.g. proteins)) as well as factors relating to the membrane (porosity, thickness, physiochemical properties (hydrophilicity, lipophilicity)) (Malhotra and Majumdar 2001).

From a formulation point of view, the formulation factors are arguably the most critical category to consider due to patient safety. Increasing the concentration of drug in question has found to increase the bioavailability of the active; hence, improving treatment. In addition, increasing particle size or using suspensions (for poorly soluble drugs) has provided sustained drug release. However, there is a maximum particle size which can be utilised (10 $\mu$ m) before reflex tear production is triggered as a result of "foreign matter" detection (Aldrich, et al. 2013). Increased viscosity of formulations prolongs product residence time in the conjunctival sac; providing a more sustained release. However, an increase in viscosity can result in blurred vision; causing inconvenience to the patient (Hiraoka, et al. 2012). Other approaches for extended- drug delivery involve altering the pH and the tonicity of ocular formulations, resulting in higher drug bioavailability (Gupta, et al. 2010; Reddy and Ahmed 2013; Suresh and Abhishek 2016).

One major hurdle met by formulation scientists regarding ocular drug delivery is the poor bioavailability of ophthalmic drugs. As a result of this, permeation enhancers (PEs) have been incorporated into formulations to increase drug absorption and in turn improve ocular bioavailability. There are five main classes of PEs; calcium chelators, preservatives, surfactants, glycosides and fatty acids. Calcium chelators like ethylenediaminetetraacetic acid (EDTA) supposedly work by interfering with the tight junctions between the superficial epithelial cells in the corneal epithelial layer; enhancing paracellular drug movement (Kaur and Smitha 2002; Morrison and Khutoryanskiy 2014).

Surfactants, unlike calcium chelators, enhance drug permeation *via* transcellular methods. It has been implied that surfactants interfere with the lipid bilayer of epithelial layers; forming micelles causing the phospholipids to be removed from the membrane. Both non-ionic and cationic surfactants have been used to increase the permeability of various ocular drugs such as prednisolone, dexamethasone, atenolol and timolol. Non-ionic surfactants such as Brij®98 and Brij® 78 have also been exploited as PE showing promising results in ocular drug delivery, highlighting the safety and efficacy of these surface active agents. One of the most common surfactants used in ophthalmic formulations is benzalkonium chloride, a cationic surfactant, usually incorporated in ocular solutions to act as preservative at very low concentrations (de los Angeles Ramos-Cadena and Spaeth 2016; Fukuda and Sasaki 2015) . The effects of this preservative have proved to be more effective in enhancing corneal permeation than other commonly used preservatives such as chlorobutanol and organomercurials. Borneol is a naturally occurring essential oil of *Cinnamomum camphora*. Although it does not fit into a defined category of PEs, it has shown potential in promoting corneal permeation of ocular drugs timolol maleate (TM) (Wu Chun-Jie, et al. 2006), dexamethasone (Yang, et al. 2009), indomethacin (Yang, et al. 2009) and ofloxacin (Yang, et al. 2009).

In an attempt to utilise PEs to increase the corneal penetration of TM, electrohydrodynamic atomisation (EHDA) was employed to fabricate drug loaded polymeric fibers containing PEs. EHDA is a versatile technique capable of producing a multitude of micro and nano sized structures for an array of application in the pharmaceutical arena (Mehta, et al. 2017b). The one-step, easily modified process has been exploited in recent years with promising results in many remits including anti-cancer therapy (Kaplan, et al. 2016; Lee, et al. 2016), protein delivery (Hu, et al. 2014; Ozcan, et al. 2016; Rasekh, et al. 2015; Zamani, et al. 2014), transdermal delivery (Khan, et al. 2014) and ocular drug delivery (Baskakova, et al. 2016; Kong and Mi 2016; Mehta, et al. 2015). The fundamental principle revolves around utilising an electrical field to atomise liquids to generate nano sized structures. Modifying the process parameters (applied voltage and flow rate) alongside the physical properties of the liquid being atomised (viscosity, surface tension, electrical conductivity) allows the process to be optimised for specific criteria. Baskakova et al successfully developed drug-loaded polyvinylpyrrolidone (PVP) or polycaprolactone (PCL) fibers to act as potential intravitreal plants (Baskakova, et al. 2016) whilst the electrospinning process has been used to produce

fibrous scaffolds for corneal tissue engineering (Kong and Mi 2016). Mehta et al successfully utilised the EHD technique to develop double-sided functionalised nano-coatings for contact lenses (Mehta, et al. 2015). Rapidly dissolving PVP was used to fabricate nanoparticulate (<100nm) and nanofibrous (<200nm) coatings demonstrating burst probe release and sufficient antibacterial activity; presenting a multi-functional drug delivery device.

In this study, four conventional PEs (**figure 1**) were selected to develop and characterise fibrous formulations of anti-glaucoma drug TM. TM-loaded PVP, Poly (N-isopropylacrylamide) (PNIPAM) (collectively termed as composite in this study, used at 1:1 ratio) fibers containing various permeation enhancers were synthesized using EHDA technology (electrospinning) and were evaluated using various thermal, spectral and *in vitro* models. In addition model fitting provided an insight into potential TM release mechanism from the various fiber systems. This study is one of the first of its kind; utilising the electrospinning process in conjunction with soft contact lenses to develop a novel drug delivery device for the treatment of glaucoma.

## Materials and methods

### **Materials**

PVP ( $4.4 \times 10^4$  g/mol) was obtained from Ashland (Worcestershire, UK). PNIPAM ( $2 - 4 \times 10^4$  g/mol), Ethanol (>99.9%), timolol maleate (TM,  $\geq 98\%$ ), benzalkonium chloride (BAC), ethylenediaminetetraacetic acid (EDTA), Borneol, and Brij<sup>®</sup> 78 were all supplied by Sigma Aldrich (Dorset, UK). PureVision<sup>®</sup> (Balafilcon A) silicone hydrogel contact lenses used in this study were manufactured by Bausch and Lomb (New York, USA). All reagents were of the analytical grade.

### **Solution preparation**

Base solutions containing 5%w/v (PVP-PNIPAM, 1:1 ratio) dissolved in ethanol were prepared (termed hereafter). Two different TM concentrations (5%w/w and 15%w/w of polymer weight) were prepared using the base solution. These solutions were used to prepare four further formulations based on selected PE addition (using maximum safety concentrations, giving rise to eight formulations in total as shown in **Table 1**).

### **Coating Application**

Polymeric solutions were drawn into 5 mL syringes which were attached to a syringe infusion pump (Harvard Apparatus, Pump 11-Elite, USA). This pump enabled the flow of the polymer-drug-PE solution to be controlled throughout the atomisation process. The solution was infused through silicone tubing to a single stainless needle (inner diameter: 1.6mm) at flow rates ranging between 8 and 15  $\mu\text{L}/\text{min}$  (**Table 1**). The working distance was kept at 8cm for all formulations. This set-up was connected to a high power voltage supply (Glassman High Voltage Supply, UK). The EHDA process was performed at ambient conditions (23°C). Final %w/w composition of electrospun fibers have been summarised in **table 2**.

Preliminary studies were carried out to determine the optimum working distance (between collection plate and needle) as this can affect morphology of atomised structures. The formulations were atomised and collected on microscope slides for primary analysis and were subsequently coated onto dehydrated commercial contact lenses (PureVision® silicone Hydrogel contact lenses). Controlled deposition of atomised formulations was achieved through the use of a novel lens holder device; holding up to 4 lenses) (**Figure 2a**). Masks were fabricated which enabled deposition onto peripheral regions of lenses whilst keeping the central regions uncoated, for not to obstruct vision. To determine the mass of each coating, the lenses were weighed before and after deposition.

### ***Coating Characterisation***

#### *Imaging*

Digital images of uncoated lens and coated lens were taken. Electrospun Samples were initially analysed using scanning electron microscopy (SEM) to study the size and morphology of the structures yielded from the EHDA process. Prior to assessing coated microscope slides; the samples were sputter coated with gold (S150B, Edwards, Crawley, West Sussex UK) under vacuum to prevent charging. SEM images were captured using a Zeiss Evo HD-15 at a working distance of 12mm at x50k magnification.

#### *Contact Angle Measurements*

Phosphate Buffer Saline (PBS), pH=7.4, was used to evaluate contact angle measurements on electrospun samples. The medium displays similar drug-release properties to tear fluid and has been used as a test-medium for ocular delivery systems (Jafari, et al. 1998). Contact angle

measurements were performed using a ThetaLite TL100 contact angle goniometer; with data analysed using OneAttension software. 10 $\mu$ l PBS droplets were used. Each sample was analysed 3 times at predetermined time intervals in sessile drop mode and an average was obtained.

#### *Thermal Characterisation*

The thermal properties and stability of the atomised coatings using two thermal analytical techniques; differential scanning calorimetry (DSC) and thermogravimetric analysis (DSC). DSC studies were carried out using a Jade differential scanning calorimeter (Perkin Elmer, US); 2-4mg of sample were hermetically sealed in aluminium pans were heated at a rate of 20°C/min from 20° to 200°C, under purge and flow of nitrogen gas.

#### *FTIR Spectroscopy*

Fourier transform infrared spectroscopy (FTIR) was used to assess any potential interactions between the drug, polymer and permeation enhancers. The electrically atomised samples as well as raw materials were scanned over the range 400-4000cm<sup>-1</sup> using FTIR Platinum-ATR fitted with Bruker Alpha Opus 27 FT-IR at an average of 10 scans at resolution 4cm<sup>-1</sup> at ambient temperature.

#### *Drug Release Analysis*

For *in vitro* drug release studies, a specific lens holder for coated lenses was designed to carry the lens whilst enabling surface contact with release medium (Phosphate Buffer Saline (PBS), pH=7.4) via cellophane dialysis membrane. Upon fixation of lens into holder; the entire device was inserted into vials containing 10mL of PBS at physiological conditions (pH=7.4, 37°C) which was constantly stirred (90 rpm). At predetermined time points, 1mL of release medium was retracted and replaced with 1 mL fresh PBS. Drug release was determined using UV spectroscopy absorbance at  $\lambda=295\text{nm}$ . The study was carried out in triplicate and an average was taken. The data collected from these *in vitro* studies were plotted in various kinetic models to assess the release kinetics of TM from the atomised polymeric coatings.

#### *Probe Release in conjunction with fluorescence microscopy*

*In vitro* probe release was analysed using a similar set-up described above for *in vitro* drug release; with probe Rhodamine B replacing TM as the active being encapsulated. The lens

were placed into the lens holder and inserted into vials of PBS at 37°C. A total of 5 lenses were coated and introduced to PBS for each formulation and were removed from the vials at predetermined times (0 mins, 10 mins, 1 hour, 6 hours and 24 hours). Experiments were performed in triplicate for all formulations. UV Spectroscopy ( $\lambda=560$ ) was used to analyse the dye intensity (DI) of the release medium and fluorescence microscopy was used to determine DI on the lens.

#### *Statistical Analysis*

A one-way Analysis of Variance (ANOVA) test was carried out to compare the release of drug from polymeric NFs containing different PEs. Derived  $p$  values  $<0.05$  were considered statistically significant.

#### *In Vitro Biological Evaluation of TM-Loaded Atomised Coatings*

A Bovine Corneal Opacity and Permeability (BCOP) test was performed to study the ocular tolerability of the formulations used to produce the lens coatings. Bovine eyes were obtained from abattoirs ABP Food Group, Guildford, UK. Freshly excised bovine eyes were extensively checked for any corneal damage; undamaged eyes were taken forward for the next stage of the experiment whilst damaged eyes were appropriately disregarded. The undamaged bovine eyes were incubated for 10 minutes at  $37 \pm 0.5^\circ\text{C}$  in a shaking water bath, shaking at 90 rpm. One drop of normal saline solution was placed on the bovine cornea, before further incubation (for 5 minutes). 100 $\mu\text{l}$  of the sample (fibrous coating dissolved in PBS) was introduced to the corneal surface and left for 30 seconds. The eye was subsequently washed with 10ml of normal saline and incubated for a further 10 minutes. Any corneal damage to the cornea was evaluated visually by gauging the degree of opacification alongside using a staining method with sodium fluorescein solution (2%w/v) under a cobalt blue filter (465-490nm).

## **Results and Discussion**

This study utilised a composite polymer system; a 50:50 mixture of PVP and PNIPAM. PVP is a rapidly dissolving polymer which has been used extensively in the pharmaceutical industry. PNIPAM is a thermo-responsive polymer with great biocompatibility that can undergo reversible phase transition (swollen state to dehydrated state) above  $32^\circ\text{C}$ . PNIPAM is also

capable of swelling and expelling its contents at physiological temperature; a property that is advantageous in controlled drug delivery *via* inserts and tissue engineering in the human body (Ashraf, et al. 2016) including ocular drug delivery (Barbu, et al. 2009; Cao, et al. 2007; Lima, et al. 2016; Prasannan, et al. 2014).

**Figure 2a** shows a schematic diagram of the electrospinning system; with the stable Taylor Cone jet enabled (**Figure 2b**), which is required to produce near-uniform fibrous structures.

**Figure 2c** demonstrates an uncoated contact lens whilst **Figure 2d** shows a typical coated lens; with a radial coated region. The central transparent region is not fixed and can be easily expanded to increase the peripheral vision region. Whilst in this study the masking region was kept to a radial format; it does not have to be restricted to this. The drug loading can be increased and the thickness of the coating can also be optimised and focused on a specific region of the lens. It is also noteworthy that personalised (cosmetic) contact lenses which are currently available with graphical features do not obstruct peripheral region with even smaller transparent regions than that used in the study. While the current system will provide greater formulation-cornea contact, considerations of the system will need to be explored including impact on peripheral vision and application duration and times. Previous studies have demonstrated medicated lenses with promising results (Garcia-Millan, et al. 2015; Glisoni, et al. 2013; Mehta, et al. 2017a) but research relating to active coatings for lenses is extremely scarce.

#### *Morphology and Size Distribution*

**Figure 3** shows electron micrographs obtained from SEM analysis while **Table 3** consolidates fiber size for each formulation. As a result of incorporating PNIPAM into the formulation, the viscosity of F1-F8 increased; resulting in the production of nanofibers for (NFs) all formulations (**Figure 3**). Electrospinning PE-free formulation and F1 produced visibly beaded fibers; with some F1 fibers as small as 33nm. These could arise as a result of the working distance between the stainless steel needle exit and the collection substrate being too low. Due to this, there is insufficient space for the viscous formulation to “stretch” at the nozzle, causing inadequate solution evaporation to produce smooth fibers (Nasouri, et al. 2015). All other formulations show smooth-surface fibers. BAC-containing fibers loaded with higher concentration of TM showed much smoother fibers than those with low drug concentration

(5%w/w with respect to the polymer). The increase in drug concentration distinctly had an effect on the morphology of the electrospun fibers; however the average diameter increased to 90.32nm as result of increased drug loading. Unlike PE-free NFs, F1 and F5; the incorporation of the remaining 3 PEs produced smooth fibers. Both F3 and F7 produced smooth-surfaced NFs with bell-shaped distribution; with drug loading not altering the size of the fibers; 74.27nm and 74.30nm respectively. These fibers are much finer than those reported by Li et al when using PVP alone as a polymeric matrix. Borneol-PVP electrospun nanocomposites produced possessed smooth surfaces with an average fiber size of  $610\pm 120$ nm (Li, X., Wang, X., et al. 2012). Beaded NFs were produced when electrospinning F4 and F8, indicating an insufficient working distance as with F1 NFs. This increase in diameter is associated with the incorporation of higher drug concentration encapsulated within the fibers.

PVP has previously been electrospun to produce fibers with an average diameter of 305nm (Huang, et al. 2016). While research involving processing of TM-loaded PVP:PNIPAM formulations for ocular delivery using EHDA is scarce, TM has been electrospun into polyvinyl alcohol (PVA) and polycaprolactone (PCL) fibers; producing NF patches with fibers ranging between 200 and 400nm (Gagandeep, et al. 2014). PVP has been previously reported to produce contact lens coatings; yielding both nanoparticles (50nm-130nm) and NFs (130-250nm) (Mehta, et al. 2015). The PE-loaded NFs produced here are reportedly much thinner than those previously stated in earlier findings making use of the electrospinning technique.

#### *PBS Contact Angle Behaviour*

Contact angle (CA) (or wetting angle) is the quantified angle between a liquid-solid interface following application liquid droplet on a solid surface. CA is a critical measure in this study due to the interaction between the fibrous coatings and the lens material can determine detachment and release of coating and drug, respectively. The wettability of the surface of electrospun fibers were characterised and analysed over time using CA (**figure 4**).

Upon application of PBS droplet ( $t=0$  seconds), F2 demonstrated the highest static angle ( $79.91^\circ$ ) whilst F1 has the lowest ( $66.6^\circ$ ). This drastic reduction in CA at  $t=0$  seconds compared to formulation without any permeation enhancers ( $CA=126.27^\circ$ ) shows the addition of PE (which all act as surfactants) lowered the surface tension of the formulations and in turn of

the electrospun NFs (Stephansen, et al. 2016). This consequently increases the wettability of the samples; indicating the samples have become more hydrophilic. This difference in CA could also be due to the change in NF morphology compared to the beaded-fibers of formulations not containing PE. The presence of spherical structures with fibrous components increases the amount of air entrapped between the solid and liquid droplet; in turn pinning the motion of the water droplet as it advances, causing an increase in CA. The combination of particles and fibers in composite-TM samples (without PE) both increases surface area and surface roughness which can contribute to the increased time period required for the PBS droplet to completely disappear.

The complete spreading of water within 20 seconds demonstrates the hydrophilicity of the fibrous coatings; highlighting an affinity to the hydrophilic soft contact lenses; aiding the attachment of the electrospun coating to the lens.

It is noteworthy that the concentration of drug (5%w/w or 15%w/w with respect to the polymer) did not affect the initial CA or the CA profile. As seen in **Figure 4**, those containing the same PE displayed almost identical CA profiles over time.

#### *DSC Analysis*

Figure 5 presents DSC thermograms for all 8 formulations, including raw composite and neat drug. Pure TM is a crystalline drug with a defined melting point ( $T_m$ ) of 218°C (**figure 5**). The absence of this sharp endothermic peak in thermograms of F1-F8 indicates the drug is no longer present in crystalline form but now distributed in the amorphous format within the polymeric matrix. PVP and PNIPAM are predominantly amorphous polymers; which experience a phase transition upon temperature changes at specific thresholds. In the case of this study, during the transition, the polymer changes from brittle to ductile. (Khan, et al. 2013; Pawar, et al. 2015). The threshold at which this occurs is known as the glass transition temperature ( $T_g$ ). Whilst incorporation of solid materials (e.g. permeation enhancers) can significantly affect the  $T_g$ , our study shows there is insignificant effect of PE incorporation on  $T_g$  of the raw composite (depicted between approximately 55-65°C) in the thermograms for raw composite and all 8 formulations. The lack of change in  $T_g$  may also be as a result of weak interactions (i.e. covalent bonds) between TM and the polymeric chains (Khan, et al. 2013). The presence of the broad endothermic peak in the thermogram for each formulation is as a

result of residual solvent evaporation and also indicates the system was amorphous at the time of DSC analysis.

### *FTIR Spectroscopy Analysis*

FTIR analysis is advantageous when trying to show compatibility between different excipients in a sample. Secondary interactions such as hydrogen bonding and Van der Waals (induced dipoles) often increase the stability of structures; interactions which can be detected by shifts in wavelength ( $\text{cm}^{-1}$ ) in FTIR spectra. **Figure 6** shows the spectroscopic spectra derived from FTIR analysis of all 8 formulations and raw materials. FTIR was used to show the stability of TM when processed in conjunction with polymer and PE. Pure TM shows characteristic peaks at  $2968\text{cm}^{-1}$  (aliphatic C-H stretching),  $3063\text{cm}^{-1}$  (aromatic C-H stretching),  $1718\text{cm}^{-1}$  (C=O),  $1229\text{cm}^{-1}$  (O-H bending),  $954\text{cm}^{-1}$  (C-O stretching vibrations). These peaks are less noticeable in the spectra for all 8 formulations; with some peaks shifting very slightly. This interpretation of peaks confirms formation of hydrogen bonds with polymer and/or PE. Characteristic peak at  $1651\text{cm}^{-1}$  in all spectra for 8 formulations correspond C=O stretching vibrations in PVP. Multiple peaks at  $2948\text{cm}^{-1}$ ,  $2918\text{cm}^{-1}$  and  $2875\text{cm}^{-1}$  are present due to CH-CH<sub>2</sub> stretch vibration. Evidence of C-H deformation of cyclic CH<sub>2</sub> groups can be seen at  $1492\text{cm}^{-1}$ ,  $1459\text{cm}^{-1}$ ,  $1419\text{cm}^{-1}$  and  $1371\text{cm}^{-1}$ . Amide III bond (C-N stretching vibration), amide V (CH<sub>2</sub> rocking vibrations) and amide IV bond are present at  $1282\text{cm}^{-1}$ ,  $732\text{cm}^{-1}$  and  $648\text{cm}^{-1}$  respectively. Characteristic absorption peaks on the PNIPAM spectra included amide II bond at  $1550\text{cm}^{-1}$ , C=O stretching and CH<sub>3</sub> asymmetric stretching vibrations at  $1650\text{cm}^{-1}$  and  $2970\text{cm}^{-1}$ , respectively.

In **figure 6a**, a clear peak at  $2927\text{cm}^{-1}$  is present in the FTIR fingerprint of BAC (indicative of C-H<sub>3</sub> bending vibrations). However, this peak is less prominent in the spectra for F1 and F5; highlighting interaction between components within the sample. With samples containing EDTA, the distinctive peaks have shifted as a result of O-H groups being capable of forming hydrogen bonds with composite polymer and drug. A similar case is seen with F3 and F7 with the incorporation of borneol (**figure 6c**). With respect to pure borneol, sharp peaks at  $1054\text{cm}^{-1}$ ,  $1456\text{cm}^{-1}$  and  $2950\text{cm}^{-1}$  are observed; peaks which are absent in the fingerprint of F3 and F7. The presence of C=O bonds in PVP molecules and O-H group in borneol molecules enables them to act as proton receptor and proton donors, respectively, forming hydrogen bonds (Li, X., Wang, X., et al. 2012). Brij® 78 is also able to form hydrogen bonds with the composite

polymer and drug with characteristic peaks at  $2890\text{cm}^{-1}$ ,  $1108\text{cm}^{-1}$ ,  $1341\text{cm}^{-1}$  and  $1471\text{cm}^{-1}$  (for pure Brij® 78) being omitted from the spectra for F4 and F8 (**figure 6d**).

FTIR analysis was also carried out to observe any changes with respect to initial drug concentration. With all four PEs, the concentration of drug did not seem to have any effect on the FTIR fingerprints (**figure 6a-d**).

#### *In Vitro TM Release Analysis*

**Figure 7** shows the *in vitro* cumulative TM release from electrospun composite fibers. PE-free NFs presented a biphasic release profile; initial burst release (47% released within 10 minutes) followed by slow, sustained release; 68.24% after 24 hours. F1-F7 fibers exhibited triphasic release profile; initial burst release followed by gradual release and subsequent sustained release. The initial burst release is as a result of rapid release of surface-associated TM and PVP dissolution (Mehta, et al. 2015) with the subsequent gradual release being a result of breaking of PNIPAM polymer chains (dissolution of PNIPAM). Polymer erosion causes the 3<sup>rd</sup> phase of drug release; releasing drug in a more sustained manner with 20%-32% of the drug being released in the last 18 hours depending on PE used. Regarding F8, the release profile followed a biphasic system slow gradual release with sustained release after 6 hours. Whilst the addition of PEs slowed down the initial release and modified the release profile from biphasic to triphasic, the total amount of drug released after 24 hours increased. For example, F7 NFs released 86.71% at  $t=1440$  minutes; 18.47% more than PE-free NFs. The incorporation of PE may provide an extra barrier for drug molecule diffusion. The PE molecules may fill interfibrous voids, retarding drug diffusion through the matrix. This in turn slows the initial high burst release seen in the release from PE-free NFs.

Whilst F1-F8 released similar percentage of TM after 24 hours, the release profiles for formulations containing different PE were contrastingly different. F1 and F5 released 72% and 75% respectively after 6 hours; as opposed to F2 and F6, which released 56% and 57% of loaded TM respectively. The drastic difference (~20 %) in release could be as a result of the morphology of BAC-loaded NFs. The beaded fibers can cause uneven distribution of drug molecules throughout the polymeric fibers; resulting in burst release from the beads upon dissolution in turn releasing drug much faster than those with smooth fibers. NFs containing high TM concentration and borneol as PE released the most drug after 24 hours

(86.72%±3.09%) whilst F8 NFs released the least amount after 24 hours (77.33%±8.1%). A noticeable difference is the slow initial release of F6 compared to burst release of other formulations. After 10 minutes, 4.9% of the loaded drug had been released from F6 NFs whilst F5 fibers had released 31.1% TM. This may be attributed to the fiber size; F6 NFs had an average size of 117nm; with a majority of NFs being above 100nm. As a result of this decreased surface area, dissolution rate of NFs is slower than that of thinner fibers as with F5; hence, drug is released much slower. There was a statistical significance ( $p < 0.05$ ) difference in the release of TM from polymeric matrix containing different PEs as demonstrated by one way ANOVA; ( $F(4,55)=2.801$ ,  $p=0.0345$ ) and ( $F(4,55)=2.775$ ,  $p=0.0358$ ) for 5%w/w TM-loaded NFs and 15%w/w TM-loaded NFs respectively.

**Figure 8** exhibits the probe release data both from the electrospun coatings on contact lenses and into release medium (PBS, pH=7.4, 37°C) in order to mimic the sustained release of drug. Probe-encapsulated NFs were produced with the same composition as in Table 1; with Rhodamine B replacing TM as active. The release of dye was depicted as DI from the lens (using fluorescence microscopic images) and DI into PBS (UV-Spectroscopy; absorbance as a function of time). This study proved/confirmed the polymeric coatings do not detach from the contact lens upon exposure to release medium; ensuring sustained release of active over time.

#### *Release Kinetics*

The data from *in vitro* TM release was applied to various release kinetic models to ascertain the prominent mechanism of TM from the electrospun fibers.

The data was fitted to zero-order, first-order, Higuchi and Korsmeyer-Peppas models; with the derived regression values and relevant component values being recorded in Table 4 with corresponding plots depicted in S1.

Drug release following zero-order kinetics demonstrates a release independent to the drug concentration whilst first-order kinetics indicate the release of drug is concentration dependent. The Higuchi model is based on several premises (Higuchi 1963; Siepmann and Peppas 2011). The diffusion of the drug must only occur in one direction with the initial drug concentration in the polymeric matrix being higher than the solubility of the drug. The swelling capabilities and dissolution of the polymeric matrix must be negligible and drug

particles must be smaller than the matrix. If these criteria are met and perfect sink conditions are achieved in the release environment; the Higuchi Model can be applied to determine the dominant release mechanism.

The Korsmeyer-Peppas model is useful in situations where there may be multiple release mechanisms. A release exponent,  $n$ , determines the mechanism of drug release. **Equation 1** shows how to derive the release exponent.

$$\log\left(\frac{M_t}{M_\infty} \times 100\right) = n \log t \times \log k \quad (\text{Eqn.1})$$

Various  $n$  values depict specific release mechanisms;  $n \leq 0.45$  corresponds to quasi-Fickian drug transport,  $n=0.5$  shows Fickian diffusion (molecular diffusion of drug due to a chemical potential gradient),  $0.45 < n < 0.89$  relates a Non-Fickian diffusion mechanism,  $n=0.89$  relates to the case II transport with  $n > 0.89$  corresponds to the super case II transport (Riger and Peppas 1987) (drug transport mechanism associated with stresses and state transition in hydrophilic glassy polymers which swell in water and other biological fluids) (Korsmeyer, et al. 1983). Log cumulative release (%) was plotted as a function of  $\log t$ ; here only the first 60% was fitted to the Korsmeyer-Peppas model with resulting parameters collated from the model given in **Table 4**.

The low  $R^2$  values derived from zero-order and first order models indicated a poor fit for this type of release kinetics. Relatively high (close to 1)  $R^2$  values for all 8 formulations from Higuchi model analysis suggests TM was released via Fickian diffusion; more specifically quasi-Fickian diffusion. This derivation was further confirmed by the results from applying release data to Korsmeyer-Peppas model. F1, F2, F5 and F8 showed characteristics for quasi-Fickian release with  $n$  values less than 0.45, whilst the remaining formulations released TM via Fickian diffusion.

By collating the results from kinetic modelling, all for release kinetic models indicate the release of TM from composite electrospun fibers was predominantly diffusion-based.

#### *In Vitro BCOP Study*

The BCOP test is an *in vitro* test used to determine the toxicity of test materials. It is an organotypic assay which assesses corneal opacity and permeability to gauge the toxicity of a

sample (Abdelkader, et al. 2015; Wilson, et al. 2015). A healthy, undamaged cornea remains impenetrable to an array of materials. Consequently, any damage that affects the corneal opacity and permeability can be detected through the use of dyes under a filtered light source. **Figure 9** depicts the reaction of bovine corneal opacity to formulations F5-F8. **Figure 9a-c** demonstrates the effects of saline (negative control), acetone (mild positive control) and NaOH (positive control). Visual examination of the cornea treated with saline showed no damage whilst those treated with acetone showed a light, clouded region at the site of application (**Figures 9bi and bii**). Acetone interacts with the lipids in the layers of the cornea; causing damage to the corneal epithelial cells. This in turn can aggravate the ocular mucosal membrane; irritating the eye. With respect to NaOH, severe opacification and strong fluorescence can be observed (**figure 9c, 9f**). Upon application of NaOH to the cornea surface, saponification of the fatty acids present in corneal cell membranes is triggered. Subsequently, not only are intracellular tight junctions comprised, but the entire corneal epithelial layer. The deterioration of these junctions increases the permeation/penetration of fluorescein dye through the cornea.

The BCOP analysis revealed no damage to the cornea when exposed to formulations F5 to F8; as portrayed in **figure 9g-n** with lack of fluorescence of sodium fluorescein dye under cobalt blue light. This privation of dye penetration indicates these TM-loaded-NFs are biocompatible formulations for contact lens coatings.

### *Conclusion*

Here, we demonstrated the effects of four different permeation enhancers on the development and in vitro behaviour of timolol maleate-loaded electrospun polymeric nanofibrous coatings for contact lenses. Morphological studies exhibited smooth nanofibers for the large majority; with some formulations producing beaded-nanofibers. Thermal analysis confirmed the stability of nanofibers with differential scanning calorimetry also showing the drug was molecularly distributed in an amorphous state throughout the polymeric matrix with all 8 formulations. There were significant ( $p < 0.05$ ) differences in the timolol maleate-release profiles depending on the permeation enhancer used; with borneol presenting the most promising data for sustained release (20% more drug was released compared to permeation-enhancer-free fibers). Probe release confirmed the electrohydrodynamic engineering of nanofibrous coatings was able to adequately coat

contact lenses; enabling static interaction with the outer side of the lens. Timolol maleate release was based on quasi-Fickian or Fickian diffusion as shown by application of Higuchi and Korsmeyer-Peppas models whilst biological evaluation (using freshly excised bovine cornea) confirmed the biocompatibility of the formulations. This study focused on a daily lens design which could be worn throughout the day and removed at night. This design overcomes multiple dosing issues and limitations associated with poor drug availability. The use of electrospinning to produce contact lens coatings has not yet been explored in depth within the pharmaceutical research remit and has great potential; allowing coatings to be deposited as required with timolol maleate, but not restricted to this drug. Using electrospinning and contact lenses in conjunction proposes a novel formulation and ocular drug delivery device to enhance timolol maleate release for the treatment of glaucoma.

## References

- Abdelkader, H., Pierscionek, B., Carew, M., Wu, Z., Alany, R.G., 2015. Critical appraisal of alternative irritation models: three decades of testing ophthalmic pharmaceuticals. *Br Med Bull*, -, 1-13.
- Aldrich, D.S., Bach, C.M., Brown, W., Chambers, W., Fleitman, J., Hunt, D., Marques, M.R.C., Mille, Y., Mitra, A.K., Platzer, S.M., Tice, T., Tin, G.W., 2013. *Ophthalmic Preparations*.
- Ashraf, S., Park, H., Park, H., Lee, S., 2016. Snapshot of Phase Transition in Thermoresponsive Hydrogel PNIPAM: Role in Drug Delivery and Tissue Engineering. *Macromolecular Research*, 24, 297-304. doi: 10.1007/s13233-016-4052-2.
- Barbu, E., Verestiuc, L., Iancu, M., Jatariu, A., Lungu, A., Tsibouklis, J., 2009. Hybrid polymeric hydrogels for ocular drug delivery: nanoparticulate systems from copolymers of acrylic acid-functionalized chitosan and N-isopropylacrylamide or 2-hydroxyethyl methacrylate. *Nanotechnology*, 20, 225108. doi: 10.1088/0957-4484/20/22/225108.
- Baskakova, A., Awwad, S., Jimenez, J.Q., Gill, H., Novikov, O., Khaw, P.T., Brocchini, S., Zhilyakova, E., Williams, G.R., 2016. Electrospun formulations of acyclovir, ciprofloxacin and cyanocobalamin for ocular drug delivery. *Int. J. Pharm.*, 502, 208-218. doi: 10.1016/j.ijpharm.2016.02.015.
- Cao, Y., Zhang, C., Shen, W., Cheng, Z., Yu, L., Ping, Q., 2007. Poly(N-isopropylacrylamide)-chitosan as thermosensitive in situ gel-forming system for ocular drug delivery. *Journal of Controlled Release*, 120, 186-194. doi: <http://dx.doi.org/10.1016/j.jconrel.2007.05.009>.
- de los Angeles Ramos-Cadena, M., Spaeth, G.L., 2016. Ocular surface disease and glaucoma. *Expert Rev. Ophthalmol.*, 11, 215-226. doi: 10.1080/17469899.2016.1186545.
- Fukuda, M., Sasaki, H., 2015. The Transcorneal Penetration of Commercial Ophthalmic Formulations Containing Timolol Maleate in Rabbit Eyes. *J. Ocular Pharmacol. Ther.*, 31, 57-60. doi: 10.1089/jop.2014.0015.
- Gagandeep, Garg, T., Malik, B., Rath, G., Goyal, A.K., 2014. Development and characterization of nano-fiber patch for the treatment of glaucoma. *Eur. J. Pharm. Sci.*, 53, 10-16. doi: 10.1016/j.ejps.2013.11.016.
- Garcia-Millan, E., Koprivnik, S., Javier Otero-Espinar, F., 2015. Drug loading optimization and extended drug delivery of corticoids from pHEMA based soft contact lenses hydrogels via chemical and microstructural modifications. *Int. J. Pharm.*, 487, 260-269. doi: 10.1016/j.ijpharm.2015.04.037.
- Glisoni, R.J., Garcia-Fernandez, M.J., Pino, M., Gutkind, G., Moglioni, A.G., Alvarez-Lorenzo, C., Concheiro, A., Sosnik, A., 2013. beta-Cyclodextrin hydrogels for the ocular release of antibacterial thiosemicarbazones. *Carbohydr. Polym.*, 93, 449-457. doi: 10.1016/j.carbpol.2012.12.033.

- Gupta, S., Samanta, M.K., Raichur, A.M., 2010. Dual-Drug Delivery System Based on In Situ Gel-Forming Nanosuspension of Forskolol to Enhance Antiglaucoma Efficacy. *AAPS PharmSciTech*, 11, 322-335. doi: 10.1208/s12249-010-9388-x.
- Higuchi, T., 1963. Mechanism of sustained medication. Theoretical Analysis of rate of release of solid drugs dispersed in solid matrices. *J. Pharm. Sci*, 84, 1464-1477.
- Hiraoka, T., Yamamoto, T., Okamoto, F., Oshika, T., 2012. Time course of changes in ocular wavefront aberration after administration of eye ointment. *Eye*, 26, 1310-1317. doi: 10.1038/eye.2012.142.
- Hu, X., Liu, S., Zhou, G., Huang, Y., Xie, Z., Jing, X., 2014. Electrospinning of polymeric nanofibers for drug delivery applications. *J. Controlled Release*, 185, 12-21. doi: 10.1016/j.jconrel.2014.04.018.
- Huang, S., Zhou, L., Li, M., Wu, Q., Kojima, Y., Zhou, D., 2016. Preparation and Properties of Electrospun Poly (Vinyl Pyrrolidone)/Cellulose Nanocrystal/Silver Nanoparticle Composite Fibers. *Materials*, 9, 523. doi: 10.3390/ma9070523.
- Kaplan, J.A., Liu, R., Freedman, J.D., Padera, R., Schwartz, J., Colson, Y.L., Grinstaff, M.W., 2016. Prevention of lung cancer recurrence using cisplatin-loaded superhydrophobic nanofiber meshes. *Biomaterials*, 76, 273-281. doi: <http://dx.doi.org.proxy.library.dmu.ac.uk/10.1016/j.biomaterials.2015.10.060>.
- Kaur, I.P., Smitha, R., 2002. Penetration Enhancers and Ocular Bioadhesives: Two New Avenues for Ophthalmic Drug Delivery. *Drug Dev. Ind. Pharm.*, 28, 353-369.
- Khan, H., Mehta, P., Msallam, H., Armitage, D., Ahmad, Z., 2014. Smart Microneedle coatings for controlled delivery and biomedical analysis. *Journal of drug targeting*, 22, 790-795.
- Khan, W.S., Asmatulu, R., Eltabey, M.M., 2013. Electrical and Thermal Characterization of Electrospun PVP Nanocomposite Fibers. *Journal of Nanomaterials*, 160931. doi: 10.1155/2013/160931.
- Kong, B., Mi, S., 2016. Electrospun Scaffolds for Corneal Tissue Engineering: A Review. *Materials*, 9, 614. doi: 10.3390/ma9080614.
- Korsmeyer, R.W., Gurny, R., Doelker, E., Buri, P., Peppas, N.A., 1983. Mechanisms of solute release from porous hydrophilic polymers. *Int. J. Pharm.*, 15, 25-35.
- Lee, S.Y., Lee, J., Park, J., Lee, J., Ko, S., Shim, J., Lee, J., Heo, M.Y., Kim, D., Cho, H., 2016. Electrospun nanocomposites based on hyaluronic acid derivative and Soluplus for tumor-targeted drug delivery. *Colloids and Surfaces B: Biointerfaces*, 145, 267-274. doi: <http://dx.doi.org.proxy.library.dmu.ac.uk/10.1016/j.colsurfb.2016.05.009>.
- Li, X., Wang, X., Yu, D.G., Ye, S., Kuang, Q., Yi, Q., Yao, X., 2012. Electrospun Borneol-PVP Nanocomposite. *J. Nanomater*, 2012, 1-8.

- Lima, L.H., Morales, Y., Cabral, T., 2016. Ocular Biocompatibility of Poly-N-Isopropylacrylamide (pNIPAM). *J. Ophthalmol.*, 5356371. doi: 10.1155/2016/5356371.
- Malhotra, M., Majumdar, D.K., 2001. Permeation through cornea. *Indian Journal of Experimental Biology*, 39, 11-24.
- Mehta, P., Haj-Ahmad, R., Al-Kinani, A., Arshad, M.S., Chang, M.W., Alany, R.G., Ahmad, Z., 2017a. Approaches in topical ocular drug delivery and developments in the use of contact lenses as drug-delivery devices. *Ther. Deliv.*, 8, 521-541.
- Mehta, P., Haj-Ahmad, R., Rasekh, M., Arshad, M.S., Smith, A., van der Merwe, S.M., Li, X., Chang, M., Ahmad, Z., 2017b. Pharmaceutical and biomaterial engineering via electrohydrodynamic atomization technologies. *Drug Discov. Today*, 22, 157-165. doi: <http://dx.doi.org/10.1016/j.drudis.2016.09.021>.
- Mehta, P., Justo, L., Walsh, S., Arshad, M.S., Wilson, C.G., O'Sullivan, C.K., Moghimi, S.M., Vizirianakis, I.S., Avgoustakis, K., Fatouros, D.G., Ahmad, Z., 2015. New platforms for multi-functional ocular lenses: engineering double-sided functionalized nano-coatings. *J. Drug Target.*, 23, 305-310. doi: 10.3109/1061186X.2014.1001395.
- Morrison, P.W.J., Khutoryanskiy, V.V., 2014. Enhancement in corneal permeability of riboflavin using calcium sequestering compounds. *Int. J. Pharm.*, 472, 56-64. doi: 10.1016/j.ijpharm.2014.06.007.
- Mun, E.A., Morrison, P.W.J., Williams, A.C., Khutoryanskiy, V.V., 2014. On the Barrier Properties of the Cornea: A Microscopy Study of the Penetration of Fluorescently Labeled Nanoparticles, Polymers, and Sodium Fluorescein. *Mol. Pharm.*, 11, 3556-3564. doi: 10.1021/mp500332m.
- Nasouri, K., Shoushtari, A.M., Mojtahedi, M.R.M., 2015. Thermodynamic Studies on Polyvinylpyrrolidone Solution Systems Used for Fabrication of Electrospun Nanostructures: Effects of the Solvent. *Adv. Polym. Technol.*, 34, 21495. doi: 10.1002/adv.21495.
- Ozcan, F., Ertul, S., Maltas, E., 2016. Fabrication of protein scaffold by electrospin coating for artificial tissue. *Mater Lett*, 182, 359-362. doi: 10.1016/j.matlet.2016.07.010.
- Pawar, M.D., Rathna, G.V.N., Agrawal, S., Kuchekar, B.S., 2015. Bioactive thermoresponsive polyblend nanofiber formulations for wound healing. *Mater. Sci. Eng. C-Mater. Biol. Appl.*, 48, 126-137. doi: 10.1016/j.msec.2014.11.037.
- Prasannan, A., Tsai, H.-., Chen, Y.-., Hsiue, G.-., 2014. A thermally triggered in situ hydrogel from poly(acrylic acid-co-N-isopropylacrylamide) for controlled release of anti-glaucoma drugs. *Journal of Materials Chemistry B*, 2, 1988-1997.
- Rasekh, M., Young, C., Roldo, M., Lancien, F., Le Mevel, J., Hafizi, S., Ahmad, Z., Barbu, E., Gorecki, D., 2015. Hollow-layered nanoparticles for therapeutic delivery of peptide prepared using electrospraying. *J. Mater. Sci. -Mater. Med.*, 26, 256. doi: 10.1007/s10856-015-5588-y.

Reddy, J.S., Ahmed, M.G., 2013. Sustained Ocular Delivery of Sparfloxacin from pH Triggered *In Situ* Gelling System. *Journal of pharmaceutical sciences*, 40, 16-25.

Riger, P.L., Peppas, N.A., 1987. A simple equation for description of solute release: II. Fickian and anomalous release from swellable devices. *J. Controlled Release*, 37-42.

Siepmann, J., Peppas, N.A., 2011. Higuchi Equation: Derivation, applications, use and misuse. *Int. J. Pharm.*, 418, 6-12.

Stephansen, K., Garcia-Diaz, M., Jessen, F., Chronakis, I.S., Nielsen, H.M., 2016. Interactions between Surfactants in Solution and Electrospun Protein Fibers: Effects on Release Behavior and Fiber Properties. *Mol. Pharm.*, 13, 748-755. doi: 10.1021/acs.molpharmaceut.5b00614.

Suresh, C., Abhishek, S., 2016. pH Sensitive in Situ Ocular Gel : A Review. *Journal of Pharmaceutical Science and Bioscientific research*, 6, 684-694.

Taskar, P., Tatke, A., Majumdar, S., 2017. Advances in the use of prodrugs for drug delivery to the eye. *Expert Opin. Drug Deliv.*, 14, 49-63. doi: 10.1080/17425247.2016.1208649.

Wilson, S.L., Ahearne, M., Hopkinson, A., 2015. An overview of current techniques for ocular toxicity testing. *Toxicology*, 327, 32-46. doi: <http://dx.doi.org/10.1016/j.tox.2014.11.003>.

Wu Chun-Jie, Huang Qin-Wan, Qi Hong-Yi, Ping, G., Hou Shi-Xiang, 2006. Promoting effect of borneol on the permeability of puerarin eye drops and timolol maleate eye drops through the cornea in vitro. *Pharmazie*, 61, 783-788.

Yang, H., Xun, Y., Li, Z., Hang, T., Zhang, X., Cui, H., 2009. Influence of Borneol on In Vitro Corneal Permeability and on In Vivo and In Vitro Corneal Toxicity. *J. Int. Med. Res.*, 37, 791-802.

Zamani, M., Prabhakaran, M.P., Thian, E.S., Ramakrishna, S., 2014. Protein encapsulated core-shell structured particles prepared by coaxial electrospaying: Investigation on material and processing variables. *Int. J. Pharm.*, 473, 134-143. doi: 10.1016/j.ijpharm.2014.07.006.

## Figure Captions

**Figure 1** Structures of permeation enhancers used in this study (a) BAC, (b) EDTA, (c) Borneol and (d) Brij® 78.

**Figure 2** (a) Electrospinning Set-Up, (b) Formation of stable cone jet. Digital images of (c) uncoated and (d) coated lens.

**Figure 3** Scanning electron micrographs of coatings at x50k magnification of (a) Permeation enhancer-free atomised structures (b) F1, (c) F2, (d) F3, (e) F4, (f) F5, (g) F6, (h) F7 and (i) F8

**Figure 4** Contact angle analysis over time for formulations containing a) BAC b) EDTA c) Borneol d) Brij® 78 at two different drug loadings; 5 %w/w and 15%w/w. Digital Images of PBS liquid droplet over time of formulations containing (e) 5%w/w TM and (f) 15%w/w

**Figure 5** DSC thermograms of raw timolol maleate, raw composite and electrospun fibers (a) NFs containing BAC, (b) NFs containing EDTA, (c) NFs containing Borneol, (d) NFs containing Brij® 78.

**Figure 6** FTIR spectra for raw materials and electrospun fibers (a) NFs containing BAC, (b) NFs containing EDTA, (c) NFs containing Borneol, (d) NFs containing Brij® 78.

**Figure 7** *In vitro* cumulative timolol maleate release from electrospun fibers containing (a) 5%w/w TM and (b) 15%w/w TM.

**Figure 8** *In vitro* cumulative probe release from electrospun coatings containing a) BAC b) EDTA c) Borneol d) Brij® 78 at two different drug loadings; 5 %w/w and 15%w/w.

**Figure 9** BCOP test digital images with corresponding fluorescence images of freshly excised bovine cornea treated with (a,d) Negative control, (b,e) Mild positive Control, (c,f) positive control (g,k) F5, (h,l) F6, (l,m) F7, (j,n) F8

## Figures

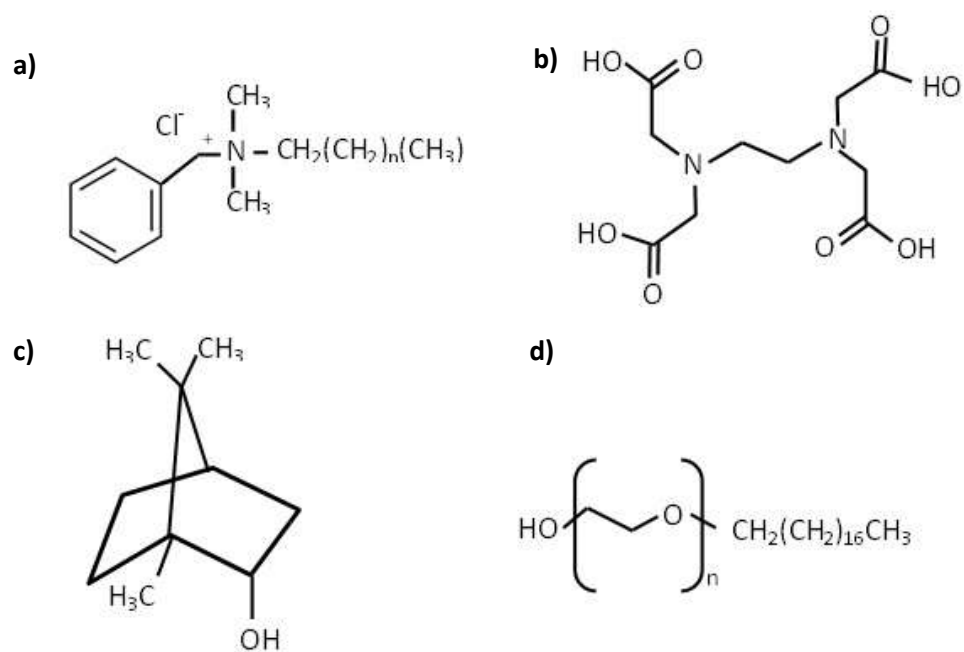


Figure 1

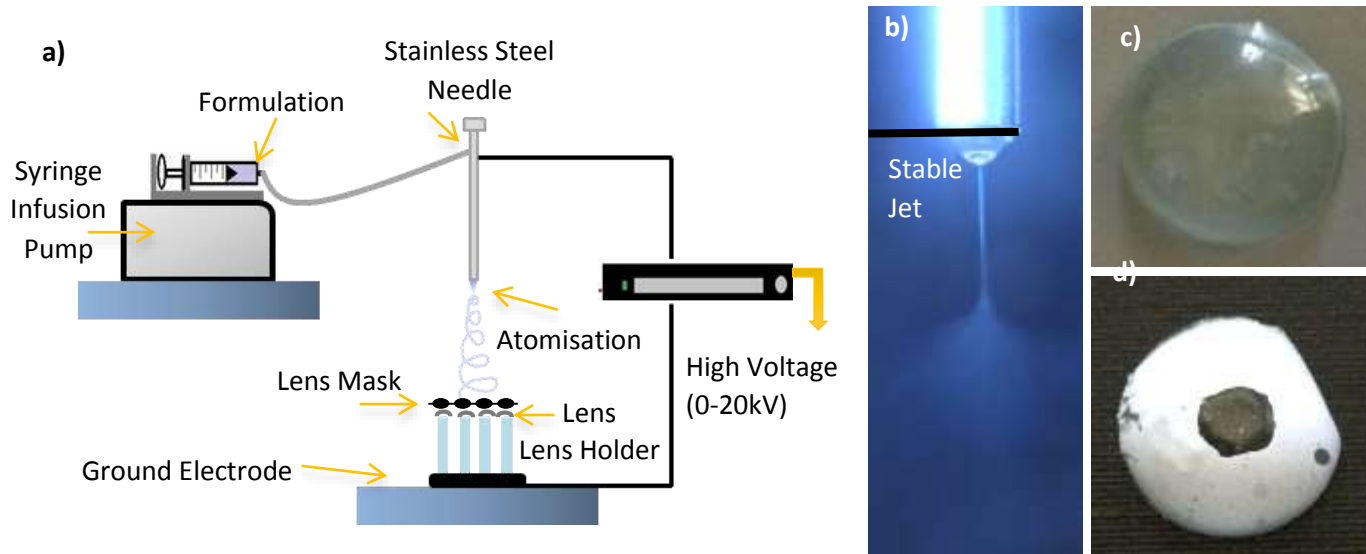
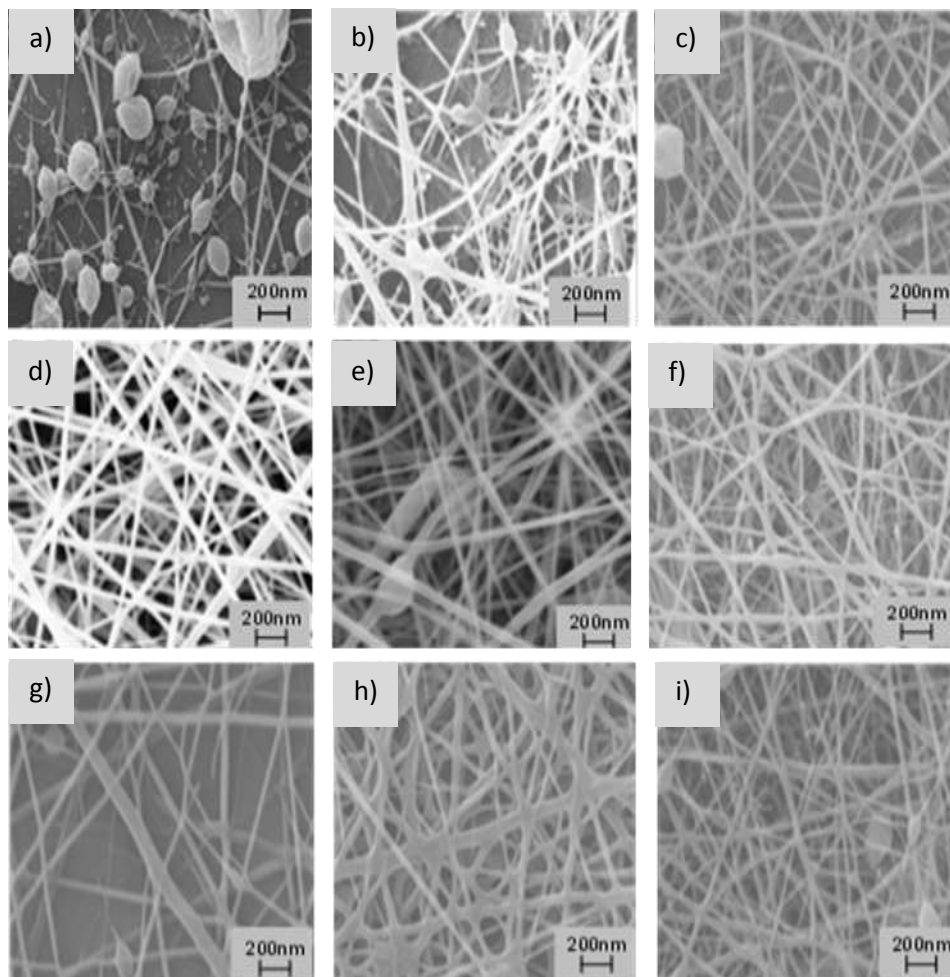


Figure 2



**Figure 3**

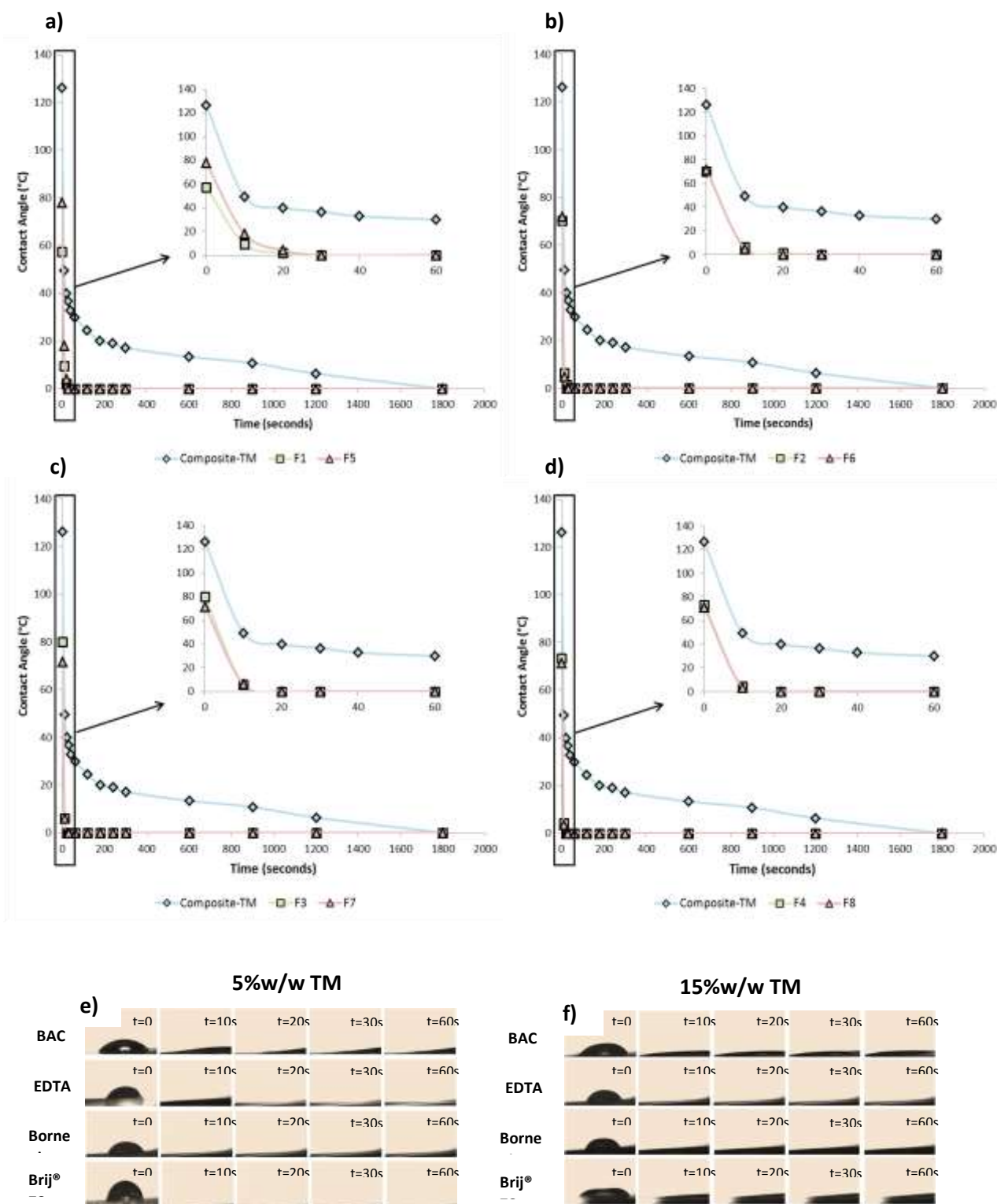


Figure 4

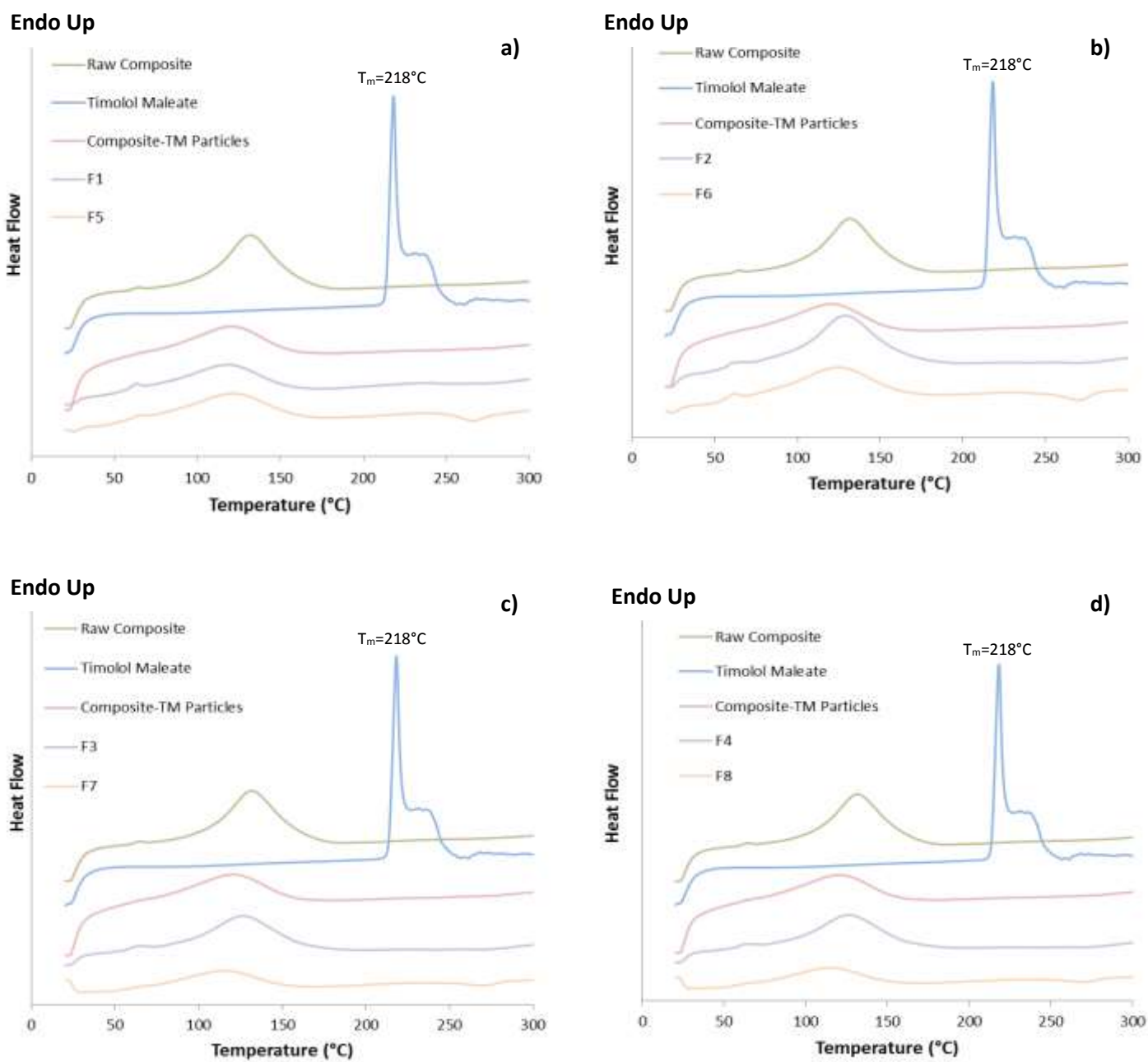


Figure 5

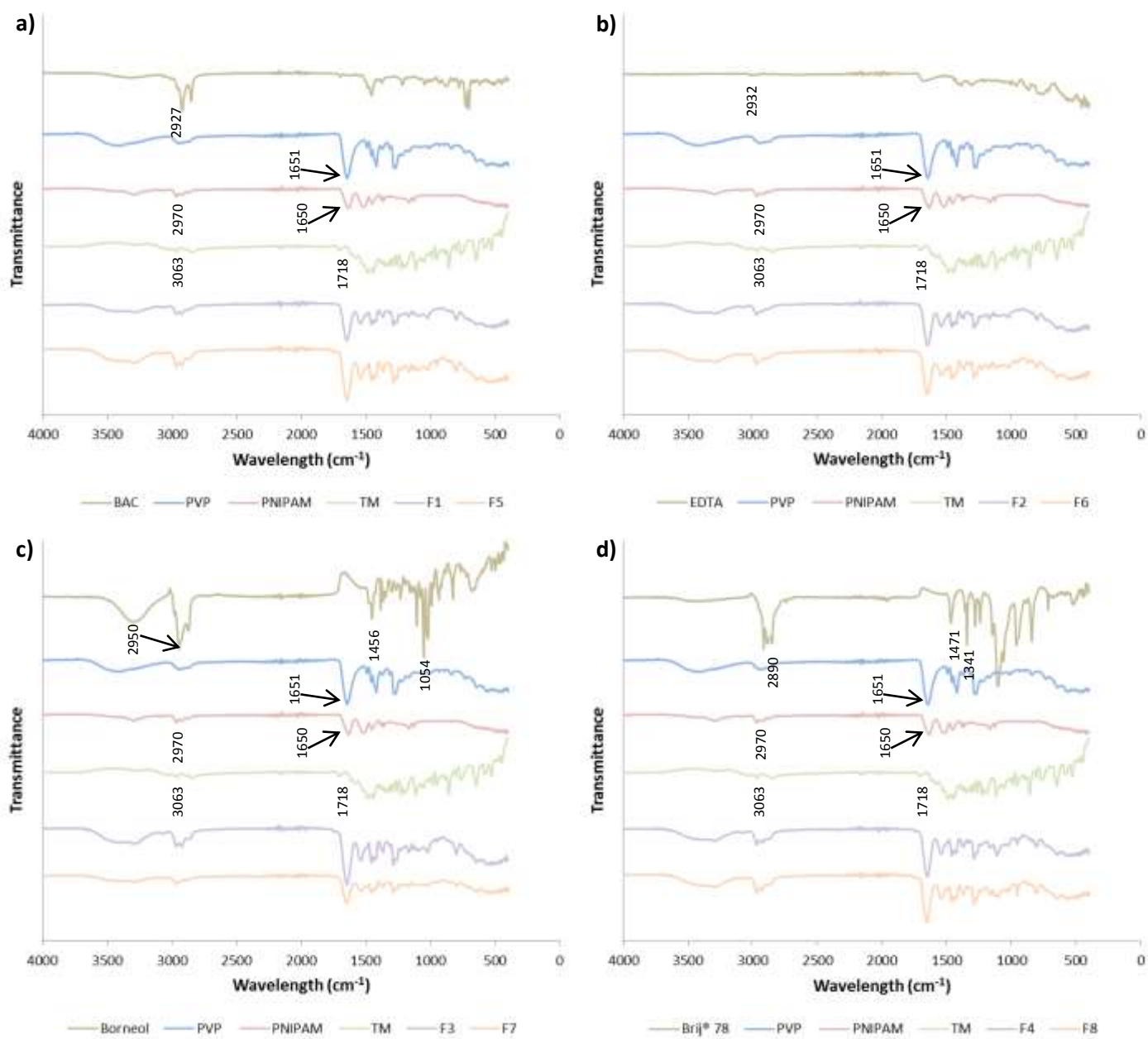


Figure 6

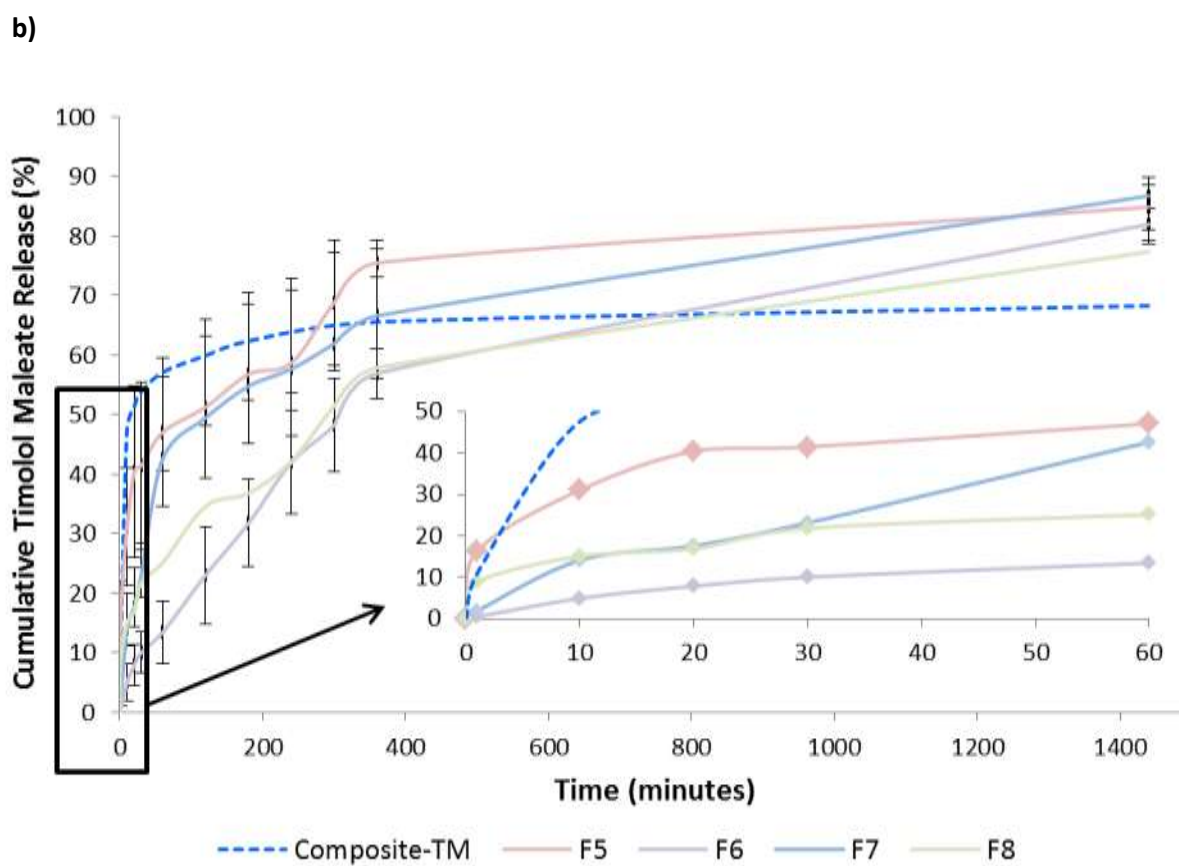
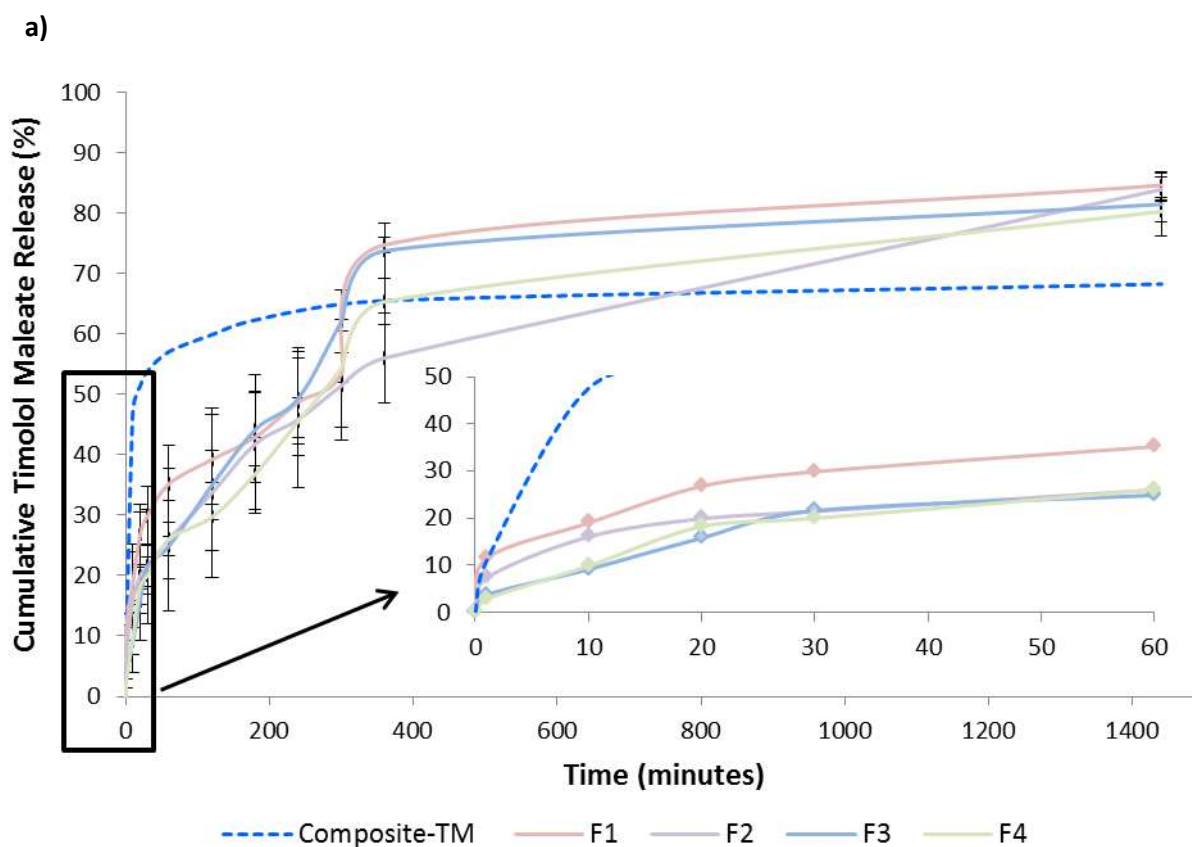


Figure 7

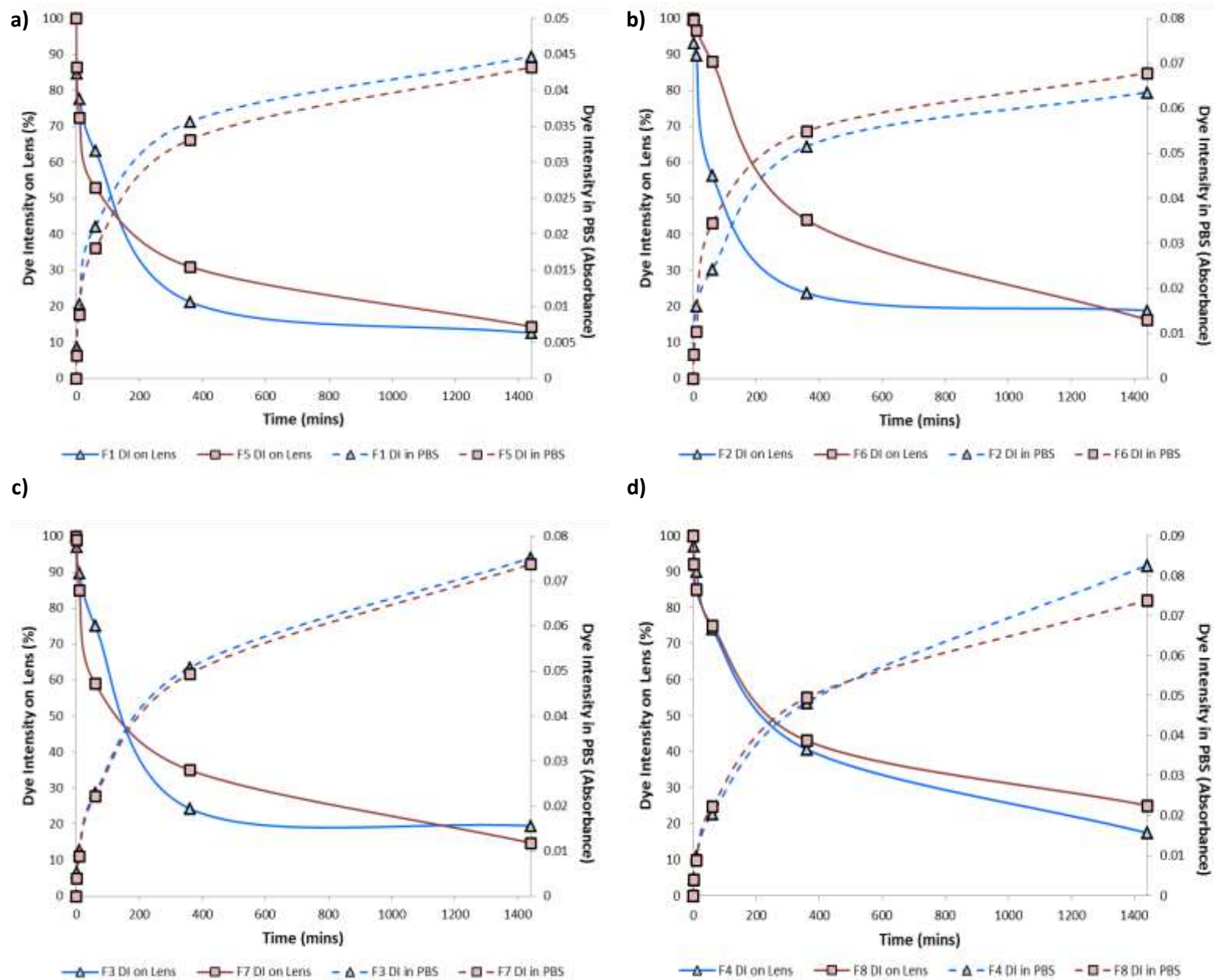


Figure 8

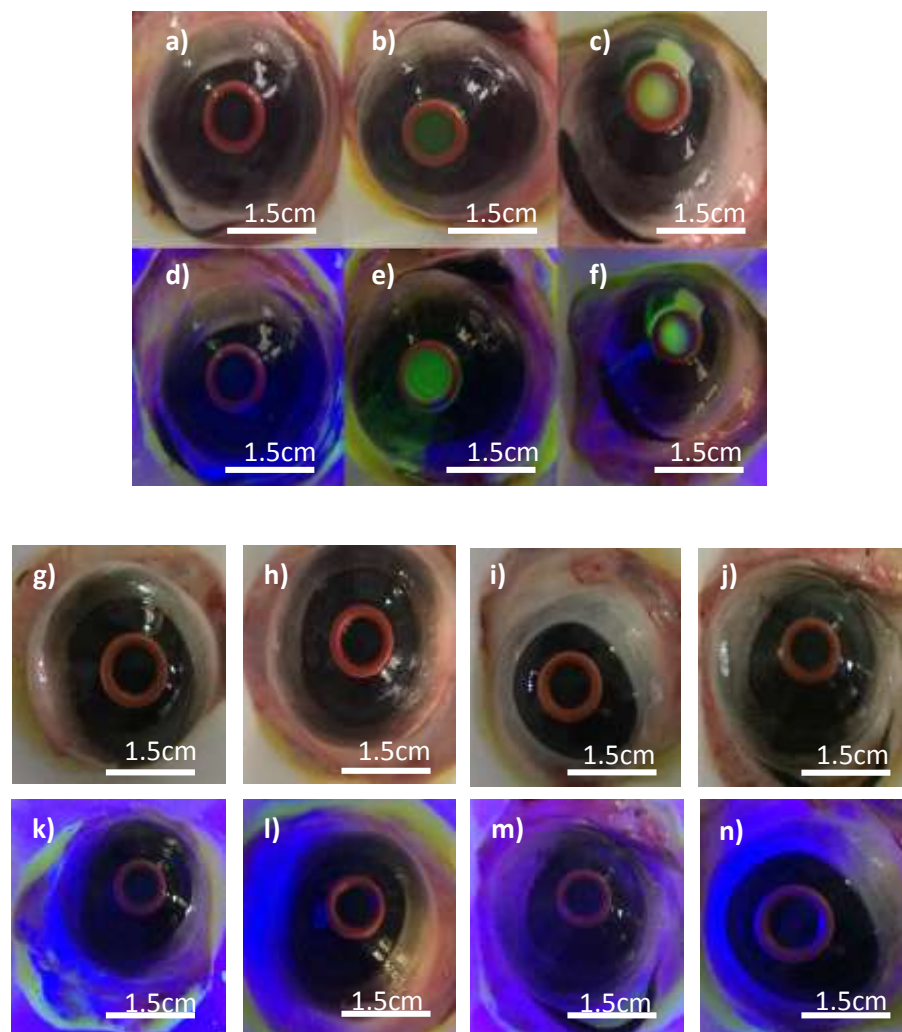


Figure 9

**Table 1** Formulation composition. Each formulation contained 2.5%w/v PVP and 2.5%w/v PNIPAM.

Formulation	TM Concentration (%w/w of polymer)	Permeation Enhancer	Permeation Enhancer Concentration (%w/v)	Flow Rate ( $\mu$ l/min)	Applied Voltage (kV)
F1	5	BAC	0.01	8	14.5
F2	5	EDTA	0.5	10	15.6
F3	5	Borneol	0.1	8	13.2
F4	5	Brij®78	1	15	14.7
F5	15	BAC	0.01	8	14.8
F6	15	EDTA	0.5	10	15.3
F7	15	Borneol	0.1	8	14.1
F8	15	Brij®78	1	15	15.3

**Table 2** Composition of Fibers (%w/w)

Formulation	Fiber Composition		
	Polymer Composite (%w/w)	Timolol Maleate (%w/w)	Permeation Enhancer (%w/w)
F1	95.05	4.75	0.2
F2	86.96	4.35	8.69
F3	93.45	4.67	1.88
F4	80	4	16
F5	86.81	13.02	0.17
F6	80	12	8
F7	85.47	12.82	1.71
F8	74.1	11.1	14.8

**Table 3** Average Fiber Diameters

Formulation	Fiber Diameter (nm)*
F1	65 $\pm$ 7
F2	56 $\pm$ 8
F3	74 $\pm$ 4
F4	80 $\pm$ 12
F5	90 $\pm$ 5
F6	142 $\pm$ 35
F7	74 $\pm$ 3
F8	118 $\pm$ 32

\*Mean  $\pm$  S.D

**Table 4** Regression Coefficients and release components derived from four different kinetic models.

Formulation	Zero Order	First Order	Higuchi	Korsmeyer-Peppas	
				R <sup>2</sup>	n
F1	0.6257	0.8135	0.88	0.9858	0.329
F2	0.7352	0.6394	0.9614	0.9948	0.339
F3	0.5858	0.7428	0.8696	0.9896	0.502
F4	0.6727	0.7592	0.9207	0.9802	0.509
F5	0.4816	0.7301	0.8357	0.9739	0.2367
F6	0.7526	0.7274	0.9537	0.9318	0.4445
F7	0.5537	0.8308	0.9561	0.9550	0.5
F8	0.6962	0.8724	0.9457	0.9756	0.319